Journal of Anatomy

J. Anat. (2009) **215**, pp506–521 doi: 10.1111/j.1469-7580.2009.01135.x

The efficacy of end-to-end and end-to-side nerve repair (neurorrhaphy) in the rat brachial plexus

Wen-Chieh Liao,[1] Jeng-Rung Chen,[2] Yueh-Jan Wang[3] and Guo-Fang Tseng[3]

[1]*Institute of Anatomy and Cell Biology, College of Medicine, National Taiwan University, Taipei, Taiwan*
[2]*Department of Veterinary Medicine, College of Veterinary Medicine, National Chung-Hsing University, Taichung, Taiwan*
[3]*Department of Anatomy, College of Medicine, Tzu Chi University, Hualien, Taiwan*

Abstract

Proximal nerve injury often requires nerve transfer to restore function. Here we evaluated the efficacy of end-to-end and end-to-side neurorrhaphy of rat musculocutaneous nerve, the recipient, to ulnar nerve, the donor. The donor was transected for end-to-end, while an epineurial window was exposed for end-to-side neurorrhaphy. Retrograde tracing showed that 70% donor motor and sensory neurons grew into the recipient 3 months following end-to-end neurorrhaphy compared to 40–50% at 6 months following end-to-side neurorrhaphy. In end-to-end neurorrhaphy, regenerating axons appeared as thick fibers which regained diameters comparable to those of controls in 3–4 months. However, end-to-side neurorrhaphy induced slow sprouting fibers of mostly thin collaterals that barely approached control diameters by 6 months. The motor end plates regained their control density at 4 months following end-to-end but remained low 6 months following end-to-side neurorrhaphy. The short-latency compound muscle action potential, typical of that of control, was readily restored following end-to-end neurorrhaphy. End-to-side neurorrhaphy had low amplitude and wide-ranging latency at 4 months and failed to regain control sizes by 6 months. Grooming test recovered successfully at 3 and 6 months following end-to-end and end-to-side neurorrhaphy, respectively, suggesting that powerful muscle was not required. In short, both neurorrhaphies resulted in functional recovery but end-to-end neurorrhaphy was quicker and better, albeit at the expense of donor function. End-to-side neurorrhaphy supplemented with factors to overcome the slow collateral sprouting and weak motor recovery may warrant further exploration.

Keywords: axotomy; brachial plexus injury; compound muscle action potential; grooming test; nerve transfer.

Introduction

Laceration or tearing of the proximal segment of nerve is not uncommon in brachial plexus injury (BPI), which severely compromises the affected upper extremity. The incidence of BPI is rather high; the World Health Organization reported incidences of obstetrical brachial plexus paralysis ranging from 0.2% to 4%, and there were around 1000 cases of traumatic injury a year in a large hospital in Taiwan (Chuang et al. 2002). Among the different methods used to reconnect injured nerve, partial transfer of selective nerve is effective in restoring elbow or shoulder function in BPI (Tung et al. 2003). With a proper donor nerve, 70–80% of the BPI patients regained elbow flexion after surgical management (Nagano, 1998). End-to-end neurorrhaphy (EEN), which uses healthy nerve as donor and unavoidably sacrifices donor function, was often preferred. An alternative, end-to-side neurorrhaphy (ESN), which promotes recipient nerve recovery and in addition preserves donor nerve function, was proposed and reported to result in successful repair of injured nerve (Viterbo et al. 1992, 1994). Although there is strong evidence that ESN results in collateral sprouting of the donor nerve and, consequently, reinnervation of the targets, the mechanisms of reinnervation and applicability in various types of injuries remain debatable (for a review see Beris et al. 2007). It also remains to be ascertained whether innervation developed by growth of sprouting from intact axons could be as effective as regeneration from axotomized donor axons and whether ESN is suitable for repairing motor nerve that controls powerful muscles.

In comparing the effectiveness of ESN vs. EEN, a detailed evaluation on the same animal nerve model is desirable. Time course and recovering capacity of both motor and sensory components of the injured nerve are critical to the

Correspondence
Dr Guo-Fang Tseng, Department of Anatomy, Tzu Chi University No. 701, Sec. 3, Jhongyang Rd., Hualien, Taiwan 97004. T/F: + 88 6 3 8564641; E: guofang@mail.tcu.edu.tw
Dr. Yueh-Jan Wang, Department of Anatomy, Tzu-Chi University No. 701, Sec. 3, Jhongyang Rd., Hualien Taiwan 97004. T/F: + 886 3 8564641; E: chris@mail.tcu.edu.tw

Accepted for publication *3 July 2009*
Article published online *7 August 2009*

choice of repair and the outcome of functional restoration. In this study, we chose to study the neurorrhaphy of musculocutaneous nerve (McN) to ulnar nerve (UN) in rats because both nerves originate from C5–T1 spinal cord segments, carry similar functional components and, most importantly, the reinnervation can be easily assessed functionally, as McN innervates the biceps brachii, which flexes the elbow joint. This experimental design conforms to the advantageous conditions suggested previously for nerve transfer (Ulkur et al. 2003). We have assessed the recovery capacity of EEN and ESN using morphological, electrophysiological and behavioral means.

Materials and methods

Adult male Wistar rats (200–300 g) were housed and cared for according to the guidelines of the College of Medicine of National Taiwan University and Tzu-Chi University. All efforts were made to minimize the number of animals used and their suffering during and after surgery and also during the invasive

Table 1 Number of animals examined following EEN and ESN

	Animal treatment group								
	EEN				ESN				
Types of examinations	1 month	2 months	3 months	4 months	2 months	3 months	4 months	6 months	Normal
Retrograde tracing of innervating neurons	–	6	6	6		6	6	6	4
Anterograde tracing of sensory fibers		6	6	6		6	6	6	4
Nerve fibers in the reconnected nerve: semithin sections	–	4	4	4		4	4	4	4
CMAP recording	4	4	4	4	4	4	4	4	
Grooming Test	6	6	6	6	6	6	6	6	6

For CMAP recording, corresponding contralateral nerves of two each of the EEN-2, EEN-3 and EEN-4 months animals were pooled and served as control.

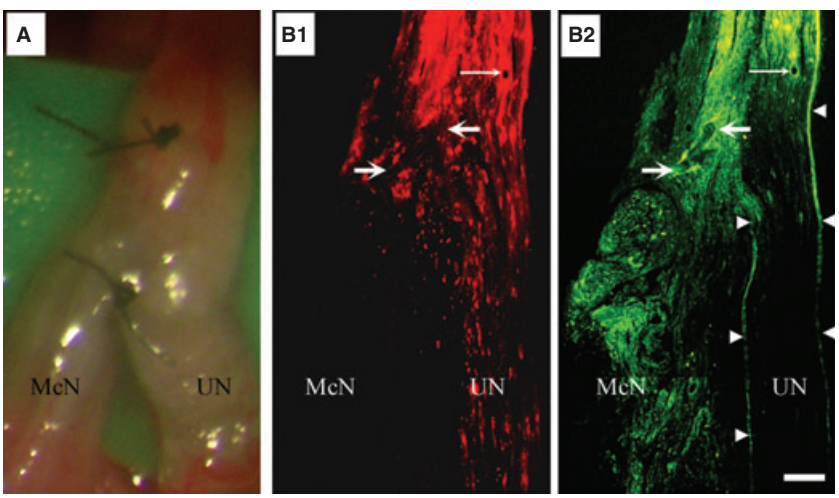

Fig. 1 ESN of McN to UN. (A) Low-power photograph of the nerves following ESN under a stereoscope during surgery. Note that the suture was on superficial structures of the nerve. B1 and B2 are a pair of montages of low-power fluorescence micrographs of a longitudinal section of the neurorrhaphied McN and UN. UN axons were labeled by applying retrograde tracer DiI (B1, red fluorescence) from its far distal part at the time of neurorrhaphy and nerve fibers that grew into the recipient nerve were labeled retrogradely with FB (yellowish green fluorescence) from the recipient nerve 4 months following ESN. Note the continuation of yellowish-green fluorescence structures from proximal UN to the coaptated McN (B2), demonstrating the growth of nerve fibers from the presumably intact donor nerve into the recipient. The pair of fine arrows in B1 and B2 point to a cross-sectioned blood vessel, thick arrows point to the suture and arrowheads in B2 outline the epineurium. Bar = 360 μm for A and 130 μm for B1 and B2.

compound muscle action potential (CMAP) recording. The numbers of animals studied are listed according to treatment and survival in Table 1.

EEN

Rats were anesthetized intraperitoneally with 7% chloral hydrate (4.5 mL kg^{-1}; Merck, Darmstadt, Germany). A longitudinal incision of the upper arm along the left mid-clavicular line was made to expose the brachial plexus. With the pectoralis major retracted, UN and McN were revealed and transected at the margin of the pectoralis major. The end of the proximal UN was then neurorrhaphied to the end of the distal McN (Oberlin et al. 1994) with 10-0 nylon sutures (Ethilon, Edinburgh, UK) under a surgical microscope. The wound was closed with 5-0 silk and animals allowed to survive for 1–6 months following surgery (Table 1).

ESN

Animals were prepared and operated as the previous group but without transecting the UN. An epineurial window matching the size of McN was slit open on the UN, taking care not to damage its containing axons, so that the cut end of McN could be attached (Fig. 1A). Animals were allowed to survive 1–6 months following surgery (Table 1).

Retrograde labeling of spinal motoneurons and dorsal root ganglion neurons

To label spinal motoneurons and dorsal root ganglion (DRG) neurons, the tip of a glass micropipette was touched with the retrograde tracer 1,1′-dioctadecy1-3,3,3′,3′-tetramethylindocarbocyanine perchlorate (DiI, Molecular Probes, Eugene, OR, USA). In EEN animals, the tracer was then placed at the cut end of UN and allowed to stand for 5 min before connecting UN to the recipient nerve. In ESN animals, the tracer was applied to UN at a location at least several millimeters below the intended coaptation site. This labeled ulnar motoneurons in the spinal cord and sensory neurons in the corresponding DRGs. To find out how many motoneurons and DRG neurons traveled into the recipient nerve after a given survival interval, the McN of animals intended to be sacrificed at 4 days was exposed and a minute amount of hydroxystilbamidine methanesulfate (Fast blue, FB, Molecular Probes) was applied to the tip of a glass micropipette and inserted into the distal part, as far as it could be identified, of the repaired McN. The glass micropipette was allowed to stay for 5 min and petroleum oil was used on the application site to prevent the leakage of the applied tracer, as it was hygroscopic.

Anterograde labeling of sensory fibers

To investigate sensory innervation, the anterograde tracer dextran conjugated with tetramethylrhodamine and biotin (10 kD, Molecular Probes) was chosen because it could be visually identified during application and observed at the end of the experiment with fluorescence or following amplification with the standard avidin–biotin method (Wang et al. 2000). For application, the tracer, which was flaky when dry, was applied by touching it to the tip of micropipette moisturized with water vapor, for instance, over hot water, as it was highly hygroscopic. It condensed into a gluey ball at the end of the micropipette immediately (Tseng et al. 1996; Liu et al. 2002) and applied into the C7–T1 DRGs of animals (Table 1) 7 days before they were sacrificed.

Tissue preparation

Rats were anesthetized and perfused transcardially with 100 mL normal saline, followed by 300 mL of 4% paraformaldehyde in 0.1 M phosphate buffer (PB), pH 7.4. The C7–T1 spinal cord, biceps brachii muscle, C7–T1 DRGs of the retrograde tracer applied animals, and a 1-cm segment of the repaired nerve including the neurorrhaphy site or corresponding location of the nerve of normal rats were collected. Tissue, except that intended for plastic embedding, was cryoprotected for subsequent sectioning. To identify anterograde tracer, 3-μm-thick cross-sections of the recipient nerve were prepared. To identify retrogradely labeled motorneurons, the studied cord segment was sectioned parallel to its dorsal surface at 25 μm thickness. To identify nerve fibers and motor end plates (MEPs), the biceps brachii was sectioned longitudinally at 40 μm thickness.

Examination of the retrograde and anterograde tracing materials

Sections of the spinal cord and DRGs intended for the examination of retrograde tracers were coverslipped with buffered glycerin and examined with a fluorescence microscope with appropriate filters for viewing the fluorescence of DiI and FB. Only labeled neurons with nuclei were counted. For motoneurons, 20 consecutive horizontal sections of the spinal cord segment of each rat that covered the whole extent of where the neurons were located were examined at 200×. For retrogradely labeled DRG neurons, nuclear profiles in all sections throughout each of the ganglia examined were counted. Total number of nuclear profiles was not corrected for split nuclei, as there was uniformity in nuclear sizes and the nuclear diameters were small in comparison with the section thickness used.

For the examination of axons anterogradely labeled from the DRGs, cross-sections of the repaired nerve distal to the neurorrhaphy site were examined for the red fluorescence of the tetramethylrhodamine conjugated to the anterograde tracer dextran that was applied (Wang et al. 2000). Due to the small sizes of nerve fibers and the resolution of light microscopy, the area of red fluorescence emitted by the labeled nerve fibers, as a fraction of the total cross-sectional area of the repaired nerve, was calculated and compared.

Preparation of the repaired nerve for nerve fiber counting and size analysis

The repaired nerve containing the neurorrhaphy site was divided into proximal, middle (containing the neurorrhaphy site) and distal parts. Comparable segments of UN and McN of normal animals served as controls. In addition, we sampled the comparable segments of the contralateral McNs of two EEN-2, -3 and -4 month animals each as a control for the effect of surgical procedure. The specimens were further fixed in 2% osmic acid for 1 h at room temperature, dehydrated in graded alcohol and embedded in Epon 812 resin (EMS, Fort Washington, PA, USA). The plastic-embedded nerve was cross-sectioned with

glass knife at 1 μm thickness, stained with toluidine blue and examined with a light microscope. The appearance of the nerve in cross-sections and the numbers and diameters of nerve fibers it contained and the thickness of the myelin sheath associated with each nerve fiber were analyzed with a PC-based program (Freeman Image-Pro Plus, Media Cybernetics, Silver Spring, MD, USA) from digital photographs of the sections.

PGP 9.5 immunostaining and acetyl cholinesterase (AChE) histochemistry

To investigate the morphological correlates of target innervation, sections of the biceps brachii muscle were processed with protein gene product (PGP) 9.5 immunohistochemistry to reveal reinnervating axons (Chen et al. 2003; Liu et al. 2006). Sections were incubated at room temperature with 1% H_2O_2 in phosphate-buffered saline (PBS) for 1 h, followed by 10% normal goat serum in PBS for 1 h and then incubated with polyclonal antibodies to PGP 9.5 (1 : 1000; Chemicon, Temecula, CA, USA) overnight at 4 °C. Sections were then incubated at room temperature for 1 h with biotinylated goat anti-mouse IgG (1 : 200; Chemicon). After three washes with Tris buffer, pH 7.4, sections were reacted with standard ABC reagent (Vector, Burlingame, CA, USA) and subsequently with 3,3′-diaminobenzidine (DAB, Sigma, St. Louis, MO, USA) in Tris buffer. Reacted sections were then rinsed in 0.1 M PB for 10 min and incubated in AChE reaction medium containing 0.5 mg mL^{-1} acetylcholine iodine (Sigma), 0.1 M sodium acetate, 0.03 M copper disulfate, 0.1 M sodium citrate and 0.05 M potassium ferricyanide in distilled water at 25 °C for 30 min. The reaction was stopped by the addition of 0.1 M PB and sections were prepared for examination.

For analysis, the number of MEPs in each of the five consecutive sections that cut through the largest extent of each muscle was counted and the mean number of MEPs in each section was derived for each muscle and used for subsequent comparison. Whole-mount muscle preparation was not used because of the limitation of antibody penetration in PGP 9.5 immunohistochemistry.

Electrophysiological test of reinnervation

To verify functional reinnervation we measured the compound muscle action potentials generated by the repaired nerve with a Viking Quest electromyogram (Nicolet Biomedical, Madison, WI, USA) 1, 2 and 3 months after EEN and 2, 3, 4 and 6 months after ESN. These time points were selected based on trial experiments that showed no consistent electrophysiological response prior to this. Lack of responses at earlier stages was also indicated in the behavioral test described below. To conduct the test, animals were anesthetized and the biceps brachii and the nerve exposed. The repaired nerve was first visually inspected for signs of infection. A hand-held nerve locator (Vari-stim®, Medtronic, Minneapolis, MN, USA) was used to confirm whether the repaired nerve innervated the target muscle before CMAP recording; reinnervated biceps brachii will twitch upon stimulation of the recipient nerve. For CMAP recording, a stimulating electrode was placed under the nerve proximal to the coaptated site and a recording electrode inserted into the biceps brachii. The stimulation site was at least 1 cm proximal to the muscle. The nerve was stimulated with 0.2-ms-square pulses of current with magnitude increasing stepwise from 3 to 13 mA at a repetition of 0.2 Hz. Three trials at least were recorded at each stimulus. Multiple traces were recorded whenever the responses showed variations in latencies or amplitudes, which often occurred during the early months of ESN. The CMAPs of the intact contralateral McNs of animals of each treatment group were regularly checked and complete series of responses to the graded stimulus protocol tested on the experimental side were recorded from two representative animals each of the EEN-2, -3 and -4 month groups and pooled as control. Data were recorded digitally and the latency, amplitude and variability of the responses were analyzed subsequently.

Grooming test

A test to evaluate the muscle power of the forelimbs of rats (Bertelli & Mira, 1993) was conducted to find out whether and when the reconnected nerve became functional. The test consisted of spraying water over the animal's face to elicit grooming movements of the forepaws toward the head. In normal grooming, the animal raised both forelimbs, licked them and reached up behind the ears. The grooming response was graded from 0 to 5. Level 0 stands for no response; 1, flexion at elbow, not reaching the snout; 2, flexion reaching the snout; 3, reaching below the eyes; 4, reaching to the eyes; 5, reaching to the ears and beyond. Animals were tested 1, 2 and 3 months following EEN and 2, 3, 4 and 6 months following ESN and the response of the left (lesion side) forelimb noted.

Statistical test

The normality of data was verified with the Kolmogorov–Smirnov test ($P > 0.1$). One-way ANOVA followed by a post hoc Bonferroni test (PRISM, GraphPad Software, San Diego, CA, USA) was subsequently used to study statistical differences between treatment groups with significance set at a P value of 0.05.

Results

To demonstrate the success of our ESN surgery, we examined longitudinal sections of the neurorrhaphy site for the retrograde tracers applied. Figure 1B shows a representative case 4 months following ESN. The first tracer DiI was applied during the surgery to the UN-labeled donor axons (Fig. 1B1, red fluorescence), and the second tracer FB was applied to the recipient nerve 4 days before the rat was sacrificed. Note labeled nerve fibers (yellow green) from the donor that grew into the recipient nerve (Fig. 1B2). This demonstrates that donor axons sprouted effectively into the recipient nerve following ESN. Behaviorally, all the ESN rats could, like in normal animals, grasp on to the grid of the cage with the forelimb of the operated side, an important function of the ulnar nerve, after recovering from anesthesia of the surgery. This supports that the surgery did not damage any of the donor axons.

The recovery of CMAP following EEN and ESN

Indication of a successful reinnervation by the reconnected nerve in the form of nerve-controlled muscle twitches

matched the successfulness of subsequent CMAP recordings in all animals that we tested. In control nerve, CMAP responses could be evoked with moderate strength stimulus (5 mA) and the amplitudes saturated at stimulus strength not much higher than threshold (Fig. 2A, Table 2). CMAP had a fixed latency of around 1.2 ms disregarding stimulus strength. Functional evaluation of the recovery of the repaired nerve following EEN and ESN is shown in Fig. 2 and Table 2. Reinnervation was first observed in animals 3 weeks following EEN; nerve locator triggered a small twitch of the biceps brachii but CMAP responses could not be reliably recorded. By 1 month (Table 2), CMAPs of long variable latencies could be detected with moderate stimulus strength (5 mA) in two of the four animals tested, while similar-amplitude responses with latencies as short as those of controls could be reliably recorded in all four animals at higher stimulus strength (11 mA). By 2 months, the response latency improved to the control level disregarding stimulus strength (Fig. 2B) and the response amplitude improved significantly to the control level in three animals when tested with 11 mA (Table 2). By the 3rd month, the amplitudes of CMAPs to 5 mA stimulus improved further (Fig. 2C) and the mean became indistinguishable from that of the control statistically (Table 2). The variability in the response amplitudes between animals to 5 and 11 mA stimuli (large SDs, Table 2) indicates that not all animals improved to control levels. In the case of ESN (Fig. 2D–F, Table 2) CMAP could not be reliably detected until 2 months, when responses to 5 mA stimuli were small and had long and variable latencies (Fig. 2D). Higher strength stimuli evoked slightly larger CMAPs that showed minor improvement on response delay in three of four animals (Fig. 2D, 11 mA trace and Table 2). By 3 months, CAMP amplitudes remained small and latencies rather variable between animals (Fig. 2E, Table 2). By 6 months, CMAP amplitudes to both 5 and 11 mA stimuli improved somewhat but remained much smaller than that of the control; however, the response latencies in three of the four animals had improved to the control level and the group mean became indistinguishable from that of the control statistically (Fig. 2F and Table 2).

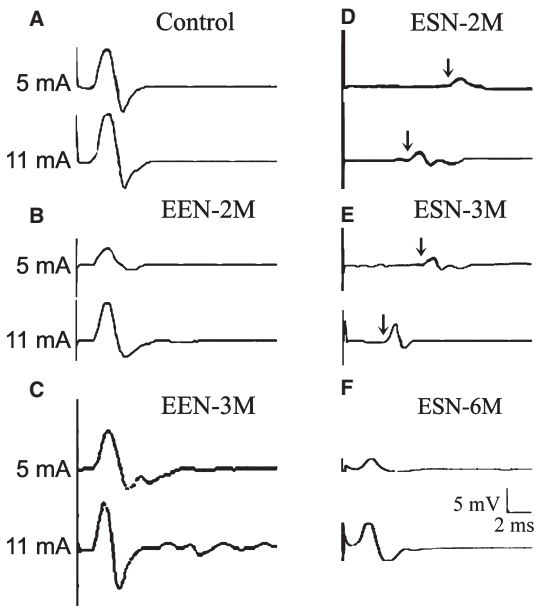

Fig. 2 Representative nerve stimulation-induced CMAPs of the biceps brachii. Each panel contains typical responses to low (5 mV) and high stimulus strength (11 mV). (A) From the contralateral control nerve of an EEN-2 months rat. (B–F) From the experimental nerve with B and C from EEN-2 months and 3 months, respectively, and (D–F) from representative animal 2, 3 and 6 months following ESN, respectively. Arrows in D and E point to the small CMAP responses recorded following a long delay after stimulation. The stimulation was delivered above the neurorrhaphy site and recording was done at the biceps brachii.

Table 2 CMAP of the studied nerve at different times following neurorrhaphy.

	Stimulus strength	Control	EEN-1 months	EEN-2 months	EEN-3 months
Amplitude (mV)	5 mA	6.08 ± 0.53	0.25 ± 0.25*	2.90 ± 1.30*	5.50 ± 4.50
	11 mA	6.90 ± 0.29	2.15 ± 0.85*	5.30 ± 3.93	7.55 ± 2.32
Latency (ms)	5 mA	1.20 ± 0.01	5.50 ± 2.50*	1.20 ± 0.01	1.20 ± 0.03
	11 mA	1.20 ± 0.01	1.20 ± 0	1.20 ± 0	1.20 ± 0
		ESN-2 months	ESN-3 months	ESN-6 months	
Amplitude (mV)	5 mA	0.31 ± 0.08*	0.70 ± 0.50*	1.60 ± 0.90*#	
	11 mA	1.15 ± 0.73*	1.10 ± 0.40*	1.60 ± 0.70*#	
Latency (ms)	5 mA	6.80 ± 2.90*	5.90 ± 2.50*	1.50 ± 0.50	
	11 mA	4.60 ± 1.38*	2.60 ± 1.40*	1.40 ± 0.58	

CMAPs were recorded from biceps brachii upon stimulating McN at the stimulus strength indicated.
Values are means ± SD.
*P < 0.05 between the marked animal and its corresponding control; #P < 0.05 between the marked animal and that of the EEN-3 months animals under a similar stimulation protocol: one-way ANOVA followed by Bonferroni tests.

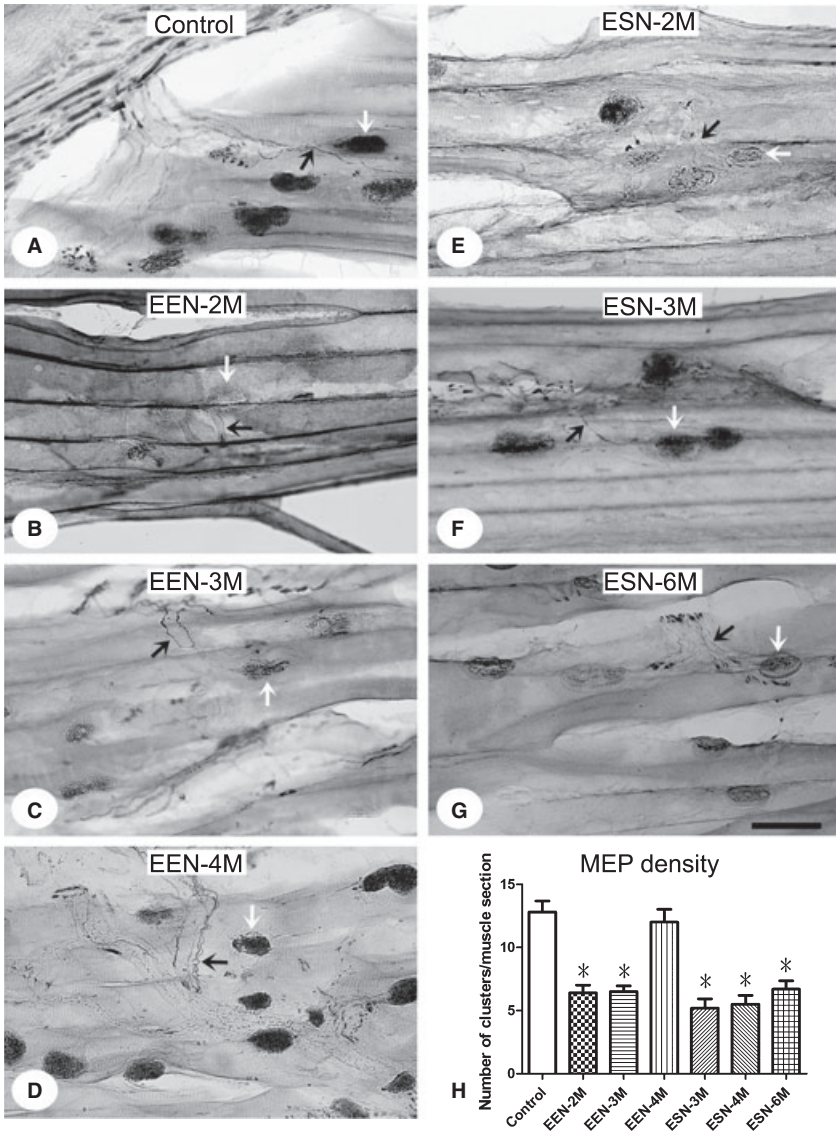

Fig. 3 Motor end plates and associated nerves of the biceps brachii. The muscle was sectioned in the longitudinal plane and treated with AchE histochemistry and PGP 9.5 immunohistochemistry to reveal MEPs (white arrows) and the innervating nerve (black arrows), respectively. Representative photos from normal (A) and neurorrhaphied rats EEN-2 (B), -3 (C) and -4 months (D) and ESN-3 (E), -4 (F) and -6 months (G) are illustrated. (H) Analysis of the densities of MEPs in each longitudinal section of the different groups studied. Data are mean ± SD. *$P < 0.05$, between the marked and the control, one-way ANOVA followed by Bonferroni post-tests. Scale bar = 50 μm.

Changes of MEPs following neurorrhaphy

Normal biceps brachii showed MEPs (AChE histochemistry; Fig. 3A, white arrows) in association with innervating nerve fiber (PGP 9.5 immunolabeling; Fig. 3A, black arrows). The density of MEPs was approximately 12.8 clusters per longitudinal section of the muscle examined (Fig. 3H, Table 3). The ratio decreased dramatically following McN transection and was restored to around control level at EEN-4 months, although it remained low, with 6.7 clusters per section at ESN-6 months (Fig. 3B–H; Table 3).

Nerve fiber growth following EEN and ESN

Temporal dynamics of fiber regeneration revealed in toluidine blue-stained, semithin cross-sections of the plastic-imbedded recipient nerves (Fig. 4) were analyzed in detail as follows.

Temporal changes in the number of nerve fibers

Normal UN contained around 50% more axons than McN (Table 4). The contralateral McNs of the EEN-2, -3 and -4 month animals contained a comparable number of nerve fibers to those of the McNs of normal animals (data not shown for brevity). The numbers of nerve fibers in the proximal and distal part of the reconnected nerve following EEN are listed in Table 4. In the proximal reconnected nerves 2, 3 or 4 months following EEN, the numbers of nerve fibers were no different from that of the normal control UN. Distal to the neurorrhaphy, the number of nerve fibers at 2 months was comparable to that of the normal UN and failed to decrease by 3 and 4 months. When comparing nerve fiber numbers proximal and distal to the neurorrhaphy, they were comparable at 2, 3 and 4 months following EEN. These indicate that EEN resulted in the regrowth, but not supernumerary sprouting, of severed donor axons.

Table 3 Data of control and experimental animals that survived for different periods of time following EEN and ESN

		EEN			ESN				
Types of examinations	Control	1 month	2 months	3 months	4 months	2 months	3 months	4 months	6 months
Ratio of double-labeled motoneurons (retrograde) (%)	98.9 ± 4.5		55.3 ± 4.6*	66.2 ± 4.8*	72.0 ± 6.3*		25.3 ± 4.6	36.2 ± 4.8*	50.0 ± 6.3*
Ratio of double-labeled sensory neurons (retrograde) (%)	99.2 ± 0.5		67.5 ± 2.1*	69.6 ± 4.7*	88.6 ± 1.2		19.3 ± 3.9*	25.3 ± 3.9*	38.1 ± 1.9*
Area ratio of anterogradely labeled sensory fibers (%)	16.5 ± 4.0		6.8 ± 2.0	18.0 ± 3.2	16.0 ± 3.5		4.2 ± 2.2	17.4 ± 2.7	17.2 ± 3.0
Ratio of small nerve fiber (diameter <1 μm) (%)	15.8 ± 2.1		13.0 ± 6.0*	18.0 ± 3.0	14 ± 1.3		4.0 ± 3.0*	3.0 ± 2.0*	10.0 ± 0.2*
Axon diameter (μm)	6.5 ± 0.6		4.0 ± 0.2*	5.2 ± 0.9*	6.4 ± 1.9		2.8 ± 1.4*	3.5 ± 1.2*	5.0 ± 1.1*
Myelin thickness (μm)	1.32 ± 0.20		0.69 ± 0.10*	0.83 ± 0.20*	1.00 ± 0.20		0.49 ± 0.20*	0.51 ± 0.20*	1.10 ± 0.50
Density of biceps brachii MEP (per section)	12.8 ± 2.7		6.4 ± 1.9*	6.5 ± 1.4*	12.0 ± 3.2		5.2 ± 2.3*	5.5 ± 2.2 *	6.7 ± 2.0*
Grooming test score	4.8 ± 0.4	3.1 ± 0.2*	3.7 ± 0.5*	4.2 ± 0.4*	4.6 ± 0.4	2.3 ± 0.5*	3.0 ± 0.6*	4.3 ± 0.5	4.8 ± 0.4

Values are means ± SD.
*$P < 0.05$ between the marked animal and its corresponding control: one-way ANOVA with Bonferroni post-tests.

Temporal changes of nerve fiber numbers following ESN were, however, quite different (Table 5). The number of nerve fibers in the donor (UN) above where the recipient nerve was attached became significantly higher than that of the control starting at 3 months following neurorrhaphy and escalated to around twice that of the control by the 6 months. Numerous sprouts grew into the proximal recipient nerve as early as 2 months and the number appeared to peak by 4 months. To find out whether nerve sprouts traveled far down the recipient nerve, we counted nerve fibers in the nerve's far distal part and found that it contained 62–80% of that of the proximal recipient nerve; this ratio increased slightly from 2 to 4 months and had reduced again by the 6th month (Table 5). Lastly, to find out whether sprouts from the donor grew specifically into the recipient nerve, we counted nerve fibers in the donor below the coaptation site (Table 5, UN: below neurorrhaphy). The number of nerve fibers remained stable at 2–4 months but increased slightly by 6 months, indicating that most, if not all, sprouted nerve fibers grew specifically into the recipient nerve (Table 5).

Nerve fiber sizes and myelin thicknesses

To find out whether and how axons altered their sizes in the process of reinnervation, we measured the diameters of those travelling distal to the neurorrhaphy (Fig. 4, Table 3); their distribution based on size is plotted in Fig. 5. In the case of EEN (Fig. 5, left column), most regenerated fibers appeared relatively thick at 2 months and their composition changed with extended survival toward smaller and medium-sized fibers resembling that of the control McN, which had a more homogeneous size distribution (Fig. 5). ESN, on the contrary (Fig. 5, right column), resulted in the predominance of small-size fibers at 2 months, which remained more or less the same by 3 months, and gradually modified so that more fibers became larger by 4 and 6 months. During the reinnervation process EEN-repaired nerve contained roughly similar numbers of presumed fine sensory fibers, < 1 μm in diameter, as the control nerve because the nerve in these stages contained about the same percentage of this category of fibers and total fibers as well (Tables 3 and 4). However, ESN-repaired nerve appeared to contain fewer of these fibers, as their percentages were considerably lower than that of the control and the nerve contained fewer total fibers, too (Tables 3 and 5).

Since axonal sizes and the thicknesses of their myelin sheath coverings are believed to reflect function, we plotted the diameters of axons against their myelin thicknesses (Fig. 6). In the control McN, the points spread evenly in the direction of the larger axon with thicker myelin. Following EEN, the points became scattered and many of them skewed to the right by 2–3 months (relatively thick axons but with thin myelin) and returned to a distribution pattern closely resembling that of the control nerve by 4 months (compare Fig. 6D with 6A). This pattern of changes was also reflected in the shifting of the slopes of the regression lines over time (Fig. 6A–D). ESN, on the other hand, resulted in the clustering of reinnervating axons in the area with small diameters and thin myelin sheath by 2–3 months (Fig. 6E,F). Note the absence of fibers in the upper right quadrant of the plot (compare Fig. 6E with 6B). Thicker axons covered with thin myelin started to appear at 4 months and some of these were covered with thicker myelin by 6 months, as manifested by the upward spread of points along the regression line (Fig. 6H). However, the distribution was quite different from that of the control nerve (compare Fig. 5H with 5A) with many data points scattered, especially far from the upper stretch of the regression line.

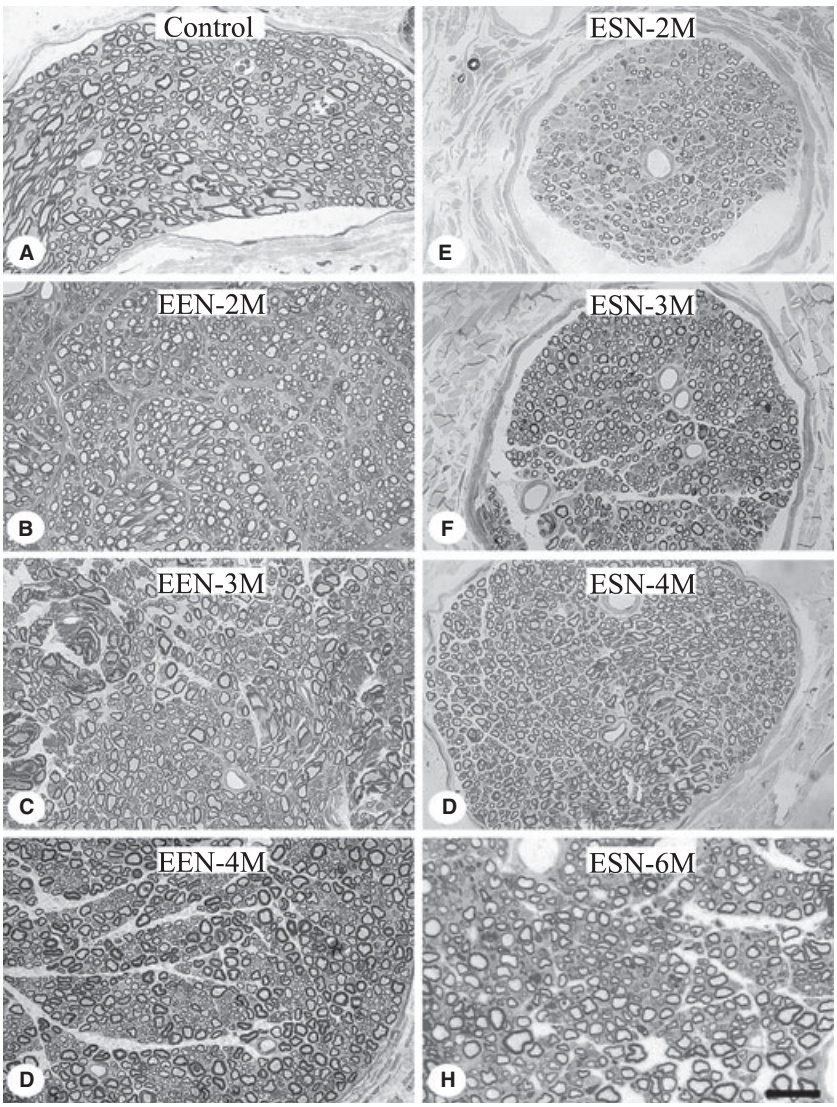

Fig. 4 Cross-sections of the repaired nerve 2 mm distal to the site of neurorrhaphy. The nerve was plastic-embedded and cut in the cross-sectional plane. Semithin sections were stained with toluidine blue. (A) Representative control McN; (B–D) the nerve 2, 3 and 4 months after EEN; (E–H) representative nerve 2, 3, 4 and 6 months following ESN. Note the dramatic reduction in axonal sizes and myelin thicknesses following ESN in particular, and the slow regaining of size by axons as survival is prolonged. Scale bar = 10 μm.

Identification of innervating motor and sensory components

Retrograde tracer DiI applied to normal or experimental animals before neurorrhaphy labeled multipolar ventral horn neurons, typical of motoneurons (Fig. 7, right column) and DRG neurons of the C7, C8 and T1 spinal segments (Fig. 8, right column). The second tracer FB introduced to the recipient nerve of EEN and ESN animals labeled neurons in locations similar to that labeled by the first tracer DiI (Figs 7 and 8, left columns). Quantitative analysis showed that, in EEN, around half of the spinal motoneurons were double-labeled, and hence were reinnervated biceps brachii, by 2 months, and the ratio increased to around 70% by 4 months (Table 3, Fig. 7), while close to 70% of DRG neurons were double-labeled by 2 months, approaching 90% by 4 months (Table 3, Fig. 8). Application of these two tracers sequentially at the same relative locations in the UN of normal rats showed that almost all neurons were double-labeled (Table 3, Figs 7 and 8) and confirmed that these two tracers were compatible with each other and that the sequential labeling method we adopted was sound. The results listed in Table 3 showed that motor and sensory neurons gradually reinnervated targets following EEN and around 72% of the motoneurons and 89% of the sensory neurons had successfully regenerated in 4 months.

In contrast, fewer motor and sensory neurons were retrogradely labeled by the second tracer applied in the animals surviving 3, 4 and 6 months following ESN (Table 3, Figs 7 and 8). The percentage of neurons regenerated by 3 months was less than half of that of the same survival EEN group. Only around 50% of the motoneurons and 38% of the DRG neurons successfully innervated the target at an extended survival of 6 months following ESN (Table 3).

Detailed examination showed that in the repaired nerve, sensory axons labeled from DRG were scattered in small groups between large bundles of myelinated fibers, which were readily identifiable under differential interference contrast optics (Fig. 9). Most of the labeled sensory fibers

Table 4 Number of fibers in normal UN and McN and the reconnected nerve following EEN

	Normal	2 months	3 months	4 months
Control UN	885 ± 293			
Control McN	576 ± 63			
Reconnected nerve, proximal to neurorrhaphy		1251 ± 155	1307 ± 451	1108 ± 60
Reconnected nerve, distal to neurorrhaphy		1239 ± 123*	1115 ± 383	891 ± 168

Total number of myelinated nerve fibers was counted from toluidine blue-stained, plastic-embedded, semithin cross-sections of the nerve segment specified.
Values are means ± SD.
*$P < 0.05$ between the marked and that of the normal McN (one-way ANOVA followed by Bonferroni test). Please see Table 1 for the numbers of animals examined in each group.

Table 5 Number of fibers in the donor and recipient nerves following ESN

	2 months	3 months	4 months	6 months
UN: above neurorrhaphy	1009 ± 263	1180 ± 183*	1133 ± 210*	2182 ± 174*#
UN: below neurorrhaphy	907 ± 151	1110 ± 276	1060 ± 228	1315 ± 251
Recipient nerve: below the site of neurorrhaphy	724 ± 328	872 ± 378	1020 ± 152	862 ± 228
Recipient nerve: far distal to neurorrhaphy	448 ± 158	699 ± 269	731 ± 182	581 ± 148

Total number of myelinated nerve fibers was counted from toluidine blue-stained, plastic-embedded, semithin cross-sections of the nerve segment specified. Proximal and distal referred to the segment of the nerve proximal and distal to the neurorrhaphy site.
Values are means ± SD.
*$P < 0.05$ between the marked and normal nerve; #$P < 0.05$ between the marked and the same segment of the nerve 2, 3 and 4 months following neurorrhaphy, one-way ANOVA with Bonferroni post-tests. Please see Table 1 for the numbers of animals examined in each group.

are presumably unmyelinated axons. Unfortunately, we could not discern individual labeled fibers due to their small sizes and therefore were unable to count them. Instead, we calculated the ratio of the area covered by labeled fibers to the total cross-sectional area of the nerve as an estimation of innervating sensory fibers. Results show that the ratio for the EEN-3 month group was comparable to that of control nerves achieved by 4 months following ESN (Table 3). Protracted survival of EEN animals to 4 months and ESN animals to 6 months failed to increase this ratio further (Table 3).

Grooming test

Analysis of the grooming movement of moving forepaw toward the head upon water sprayed over the animal's face showed that normal animals always raised both forepaws to the ears and behind to clean their face, scoring 5 on a scale of 1 to 5. In EEN, most animals were able to raise the affected paw to below the eyes (score 3) in 1 month, many of them to reach the eyes (score 4) at 2 months and some improved to score 5 by 3 months; the whole group became indistinguishable from control by 4 months (Table 3). In contrast, all ESN rats could flex their affected forelimb to reach the snout (score 2) at 2 months, and reached below and a few to the eyes (score 3 and 4, respectively) at 3 months; all animals achieved a score of 4 or 5 at 4 and 6 months (Table 3).

Discussion

This study compared the efficacy of two popular strategies of neurorrhaphy, EEN and ESN. Our key finding is that although both strategies reinstated nerve function, EEN appeared to be more efficient than ESN in both recovery time and strength of the reestablished motor force, consistent with the fact that EEN involved the regeneration of axotomized nerves, whereas ESN dealt with the collateral sprouting of intact nerves (Matsumoto et al. 1999; Akeda et al. 2006). Axotomy injures motoneurons and triggers axonal regeneration quickly (Haas et al. 1993), whereas in the case of ESN, humoral factors released by the damaged or degenerating recipient nerve are likely to play a role in activating the intact donor axons to sprout (Beris et al. 2007). These are in line with our finding that reinnervation is much faster following EEN than ESN; the presumed intact axons appeared to require a delay of around 2 months to send new sprouts that penetrated the perineurium and, through the recipient nerve, reached the target.

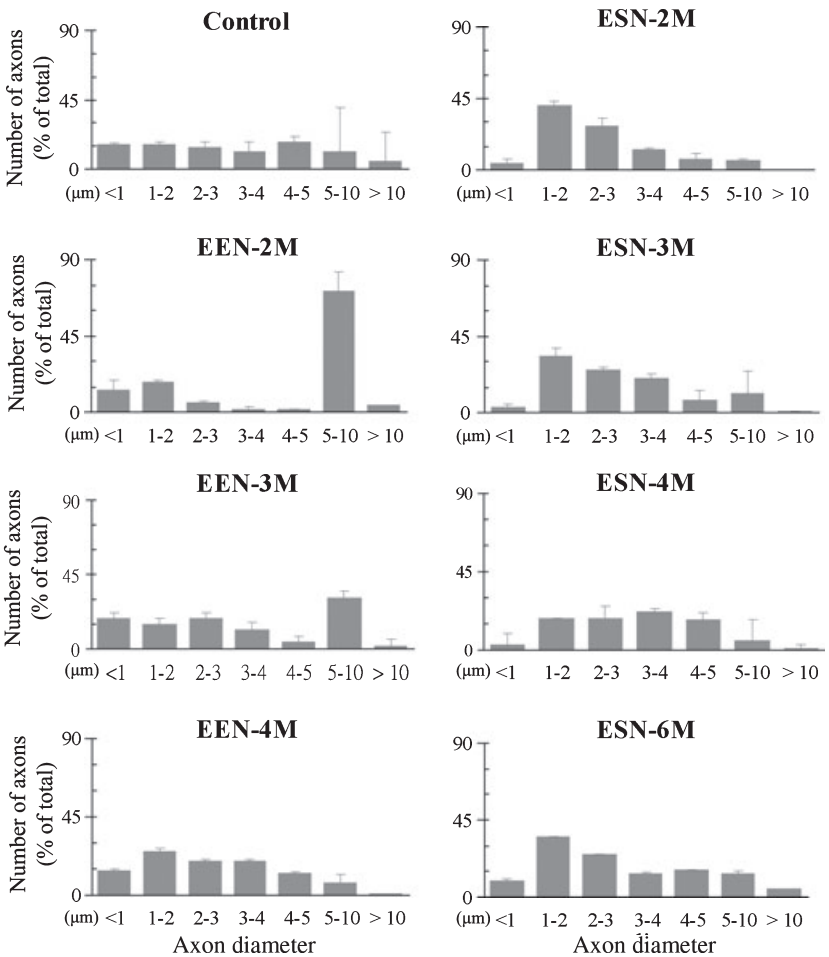

Fig. 5 Distribution of axons in the recipient nerve at different stages following neurorrhaphy. Data from control and different EEN and ESN survival animals are illustrated as labeled. Axons were grouped arbitrarily based on their diameters into different categories as shown in the abscissa. Data are mean ± SD.

On the issue of our ESN strategy, we chose to open the epineurium of the donor nerve to coaptate the recipient nerve, as previous studies suggested this enhances donor nerve sprouting (Lundborg, 2005; Zhang et al. 2006). We slit and sutured the epineurium and avoided damaging donor axons to the best of our ability (Fig. 1A). None of the donor axons appeared to be damaged, as the suture involved only superficial structures and the rats were able to grasp the cage with the forelimb of the operated side after the surgery. In this study, we found no consistent functional connection in the recipient nerve 1 month following ESN with the lack of consistent CMAP responses or nerve-controlled muscle twitches. Subsequent concurrent and gradual recovery of CMAP, density of MEP and grooming behavior and the reappearance and maturation of nerve fibers in the recipient nerve 2–6 months following ESN argue for the delayed invasion of collateral sprouts from the donor. Three additional findings indicate that donor axons took time to sprout to the new target. First, both motor and sensory donor neurons were retrogradely labeled from the distal recipient nerve starting 3 months following ESN and the increase in the percentages of double-labeling parallel that of the CMAP and MEP recovery, with up to 50% of the donor motor neurons sprouts innervating the newly acquired target. Secondly, large bundles of axons were visualized traveling from the donor nerve into the recipient nerve after applying retrograde tracer to the recipient nerve several months following ESN (Fig. 1B). Thirdly, anterograde tracing from the cell bodies of donor sensory neurons labeled nerve fibers in the distal recipient nerve as shown 3 months following ESN. Thus our physiological and morphological data support that many intact donor axons must have sprouted to innervate the new target, although the issue of whether mature intact axons can sprout to innervate a new target is still being debated (Beris et al. 2007; Hayashi et al. 2008). Experiments in rats with a silicon chamber for ESN to avoid mechanical damage to the donor nerve show clearly that intact axons could send collateral sprouts to a new target (Matsumoto et al. 1999; Akeda et al. 2006). In an elaborative study exploring the collateral sprouting of intact axons, a segment of sciatic nerve was transplanted between the left and right median nerves with different noninjurious ESN strategies in rats. Effective nerve regeneration was found consistently for both right

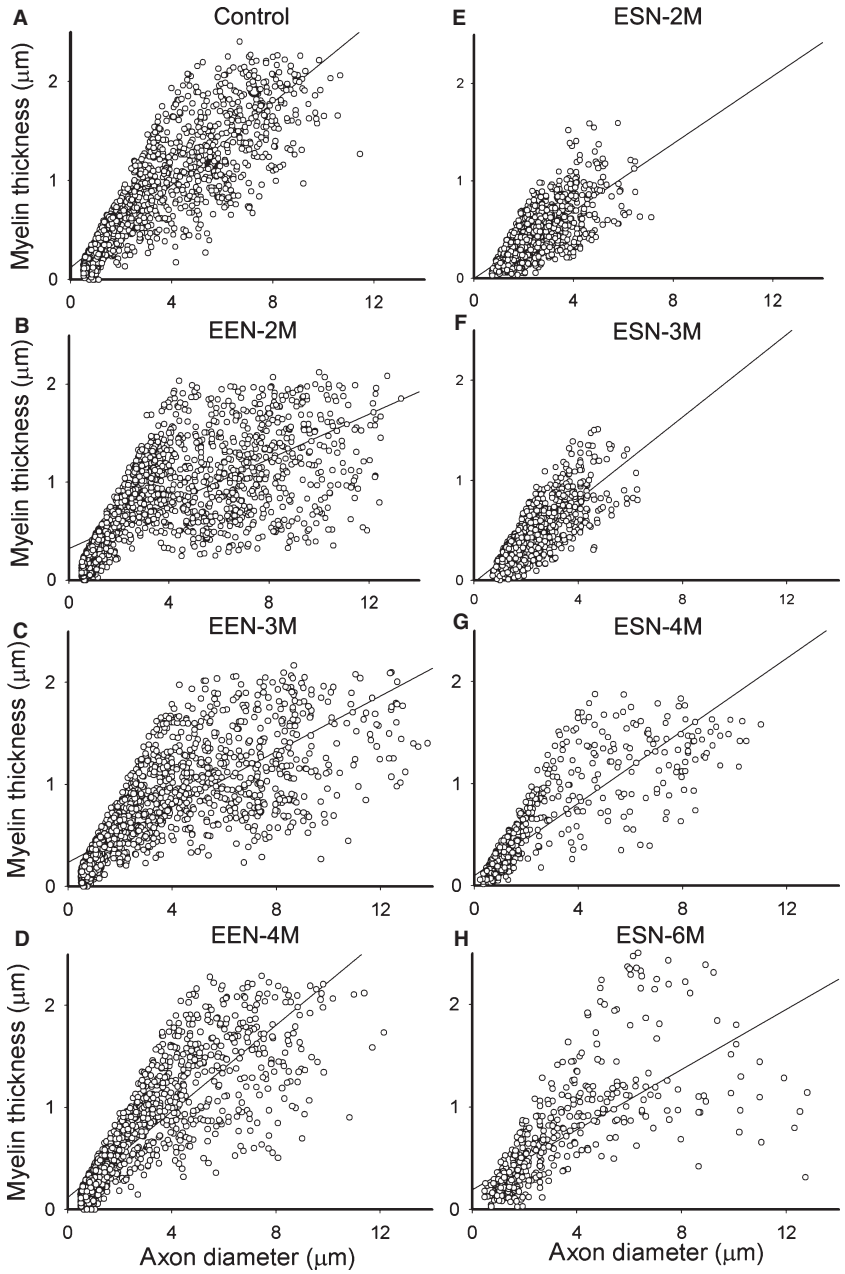

Fig. 6 Temporal changes in the relationship between diameters and myelin thicknesses of axons in the recipient nerve following EEN and ESN. Measurement was done on toluidine blue-stained plastic-embedded semithin sections. Plots of control and the repaired McN 2, 3, and 4 months following EEN and 2, 3, 4 and 6 months following ESN are shown as labeled. A linear regression line of all data points in each plot is also illustrated. Regression coefficient for the control, EEN-2, EEN-3 and EEN-4 months was 0.88, 0.78, 0.69 and 0.85, respectively, and 0.70, 0.76, 0.86 and 0.80 for the 2, 3, 4 and 6 months of the ESN groups, respectively.

and left forearm flexors contracted simultaneously upon indirect stimulation of the grafted nerve, and collateral sprouts from donor axons were visualized with confocal microscopy following fluorescence dye labeling (Hayashi et al. 2004). Thus in addition to controlling the original muscle, intact donor axons could sprout to innervate new target. In a recent retrograde labeling study of the rat McN-UN ESN model, the sensory/motor neuron innervation ratio of the coaptated nerve examined 3 months later was found to resemble that of the donor rather than the recipient nerve (Samal et al. 2006). The resemblance in neuronal traits suggests that the new innervation is derived from the intact donor axons.

Experimental strategies

Methodologically, this study dealt with EEN that transected donor nerve and used the cut end for nerve reconnection, whereas with ESN a severed nerve was attached to the epineurial window of an otherwise intact donor nerve (Bertelli et al. 1996). Although brachial axon could regenerate relatively fast, 2–4 mm day^{-1} (Stoll & Muller, 1999), and might travel for a long distance in ideal repair conditions (Bertelli & Ghizoni, 2006), induction of sprouting of an intact nerve might take longer. To take this into account, we chose McN among brachial plexus nerves as the recipient, as its axons traveled short distances from cell bodies to targets and its

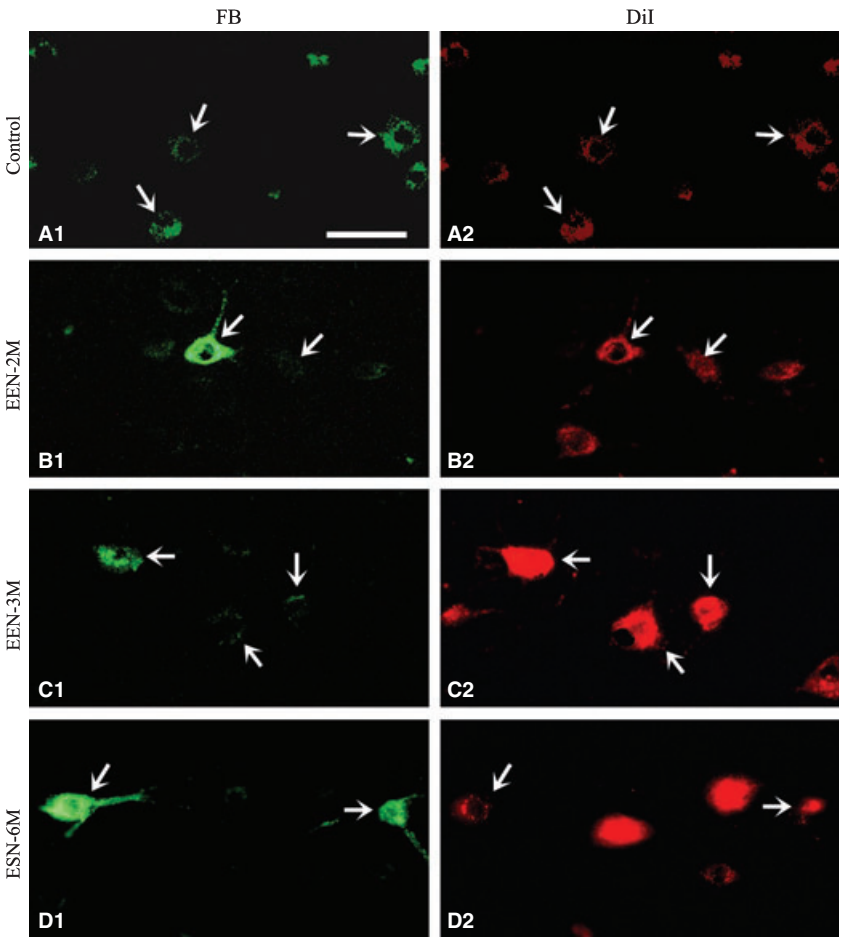

Fig. 7 Retrograde tracing of the spinal motoneurons that innervated the bicep brachii following neurorrhaphy. Representative photographs taken from horizontal sections of C7–T1 spinal cord of the studied animal are illustrated. The two photos of each row were taken from the same location of a section viewed with fluorescence filter that revealed either FB (left column) or DiI (right column). Ulnar motoneurons were labeled with the first dye, DiI, before neurorrhaphy. Those that successfully repopulated the recipient nerve were labeled by the second dye, FB, applied 4 days before the animal was sacrificed. Many motoneurons were double-labeled following neurorrhaphy (arrows). In control animals, the two tracers were applied sequentially at the same relative location as in the neurorrhaphied animals. Scale bar = 50 μm.

function could be easily evaluated. Indeed, rat McN turned out to be an appropriate choice in our hands, as axons traveled over 20 mm distal to the neurorrhaphy as early as EEN-1 and ESN-3 months. The timing of neurorrhaphy is another important issue. In clinical practice, reconnection of the injured nerve is often delayed due to the need to assess the degree of injury and signs of spontaneous recovery before invasive surgical intervention. In the present exploration we chose, on the contrary, to compare the efficacy of EEN and ESN by reconnecting the nerve a few minutes after injury for the following reasons: first, to avoid the involvement of the regression of the injured neuronal cell bodies, as injuries that require EEN or ESN were often severe (for instance root avulsion) and in animal experiments resulted in severe and progressive loss of motoneurons (Schmalbruch, 1987; Crews & Wigston, 1990); secondly, to avoid complications from muscle atrophy, spontaneous sprouting of axons and rearrangement of intraspinal circuits that might have resulted after prolonged denervation.

The efficacy of EEN vs. ESN

Changes in the size composition of the regenerated axons were different following EEN and ESN and these appeared to correlate well with the recovery patterns of CMAP and MEP as well as grooming responses.

EEN was characterized by fast recovery of CMAP responses, suggesting that axotomized donor motoneurons regenerated their axons readily and developed a robust nerve–muscle connection in a couple of months. Short-latency CMAP was detected as early as 1 month, consistent with the presence of many large-caliber reinnervating axons. These fibers appeared to decrease in size and increase their myelin thicknesses, which presumably matured further in subsequent months and consistently resulted in short-latency and high-amplitude CMAP disregarding stimulus strength. Although the donor UN contained more motoneurons than the recipient McN in our model, the developed connection was not more powerful than that of the control McN as estimated from CMAP responses. Whether our UN-McN EEN reconnected nerve could build up into more powerful connections (Guntinas-Lichius et al. 2007) with protracted survival remains to be explored.

On the other hand, ESN was typified by much slower and marginally improved CMAP responses, consistent with the delayed development of connections based on less numerous and mainly thinly myelinated small-diameter motor axons in 2 or 3 months. ESN gained fewer thickly myelinated

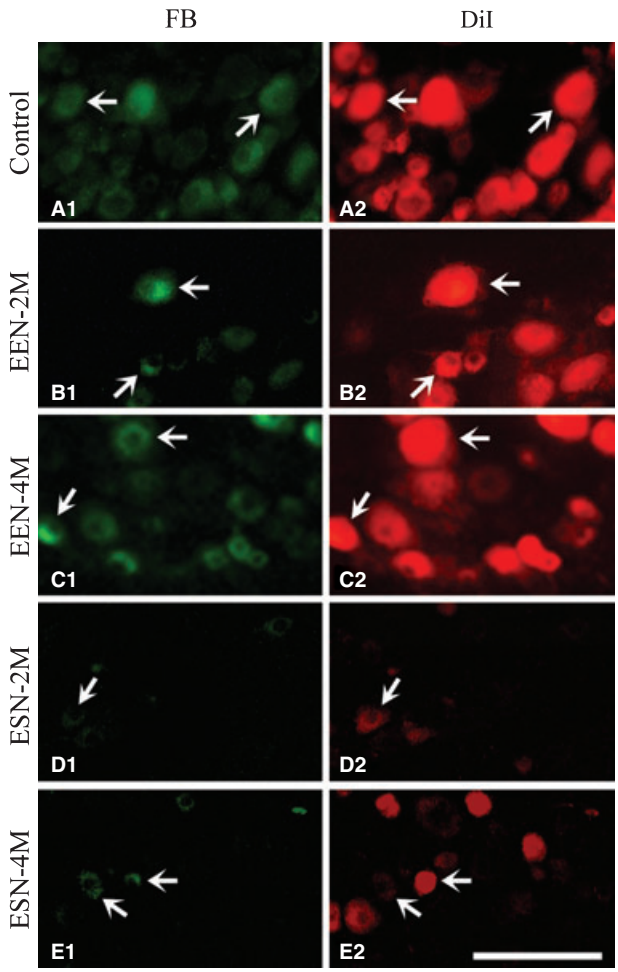

Fig. 8 Retrograde tracing of primary sensory neurons that populated the recipient nerve following neurorrhaphy. Representative labeling in the C7 DRG of control animals (A) and animals 2 and 4 months after EEN (B,C) and ESN (D,E) is illustrated. DRG neurons were labeled by the first tracer DiI before neurorrhaphy (right column). Repopulated neurons (left column) were labeled by applying the second tracer FB 4 days before sacrifice. In the control nerve, neurons were labeled using the same successive labeling paradigm. Sets of arrows in each pair of the panels show double-labeled neurons. Many repopulated DRG neurons of the EEN-4 months animals are double-labeled, as in control animals. Scale bar = 200 μm.

large fibers even with survival to 6 months. In fact, although donor nerve sprouted substantially in 2 months and profusely by 6 months, the number of nerve fibers that grew into the distal part of recipient nerve failed to increase accordingly. Differences in the time courses of CMAP and MEP recovery also indicate a slower and less efficient restoration following ESN than EEN. Based on the amplitude of the recorded CMAPs, ESN presumably restored approximately 15% of the control muscle strength in 2–3 months and 25% by 6 months, considerably less than the 60% recovery by the ESN of nerve to medial gastrocnemius to sciatic nerve (Tham & Morrison, 1998) and the 70% recovery of the ESN of median nerve to ulnar nerve (Lutz et al. 2000) in 3–4 months. Despite the relatively poor CMAP recovery, ESN animals were able to recover their upper limb grooming behavior to the control level starting at 4 months.

Motor axons appeared to regenerate nerve fiber as effectively as or slightly less than sensory fibers following axotomy, as revealed in our retrograde labeling studies following EEN. Regarding the ability of intact motor and sensory axons to sprout, an earlier study suggested that donor motor axons might respond more poorly than sensory axons to ESN, as fewer motor axon collaterals cross the donor perineurium (Matsumoto et al. 1999) and dramatically fewer motoneurons than DRG neurons were retrogradely labeled 16 weeks following ESN of rat sciatic nerve (Kanje et al. 2000). On the contrary, our retrograde labeling shows that intact motor axons might be similarly or slightly more responsive than sensory axons to sprouting following ESN. The ability of intact axons to sprout could simply be size-dependent, as motor axons are usually thicker than sensory fibers. When comparing the reinnervation of sensory fibers following EEN and ESN, our anterograde labeling suggests that they were initiated with the same efficacy, as the proximal reconnected nerve of EEN-4 and ESN-6 month rats contained a similar percentage of sensory fibers as control nerve. However, many fibers traveling into the recipient nerve might not reach the target, as there was a large discrepancy between the percentages of DRG neurons retrogradely labeled at the same times following the two neurorrhaphies.

Maturation of the reinnervation differed temporally following EEN and ESN as well. In EEN, CMAP was already detectable at 1 month, and improved to close to control by 2 months and became indistinguishable from control by 3 months. Consolidation and/or maturation of the connection following EEN was likely to have occurred during the later part of the process for the following reasons. First, retrogradely labeled motoneurons had already reached 55% of control by 2 months and had increased modestly to 72% by 4 months. Secondly, the distribution in the size and also the size–myelin sheath thickness correlation plots show that the reinnervating axons were reconfigured toward the control pattern during this time. Thirdly, the density of MEPs increased to control level by 4 months, whereas the number of nerve fibers traveling in the recipient nerve hardly changed.

In contrast, maturation of ESN-induced reinnervation was greatly delayed and was in addition complicated by a late supernumerary sprouting. The number of sprouts entering the recipient nerve peaked after 4 months and retraction and/or elimination was likely to have occurred by ESN-6 months. However, this was accompanied by a secondary boom of sprouting, indicating donor axons were likely still responsive to the coaptated nerve. However, most of the late-sprouted fibers failed to reach and enter the recipient nerve. The correlation plot between axon diameter and

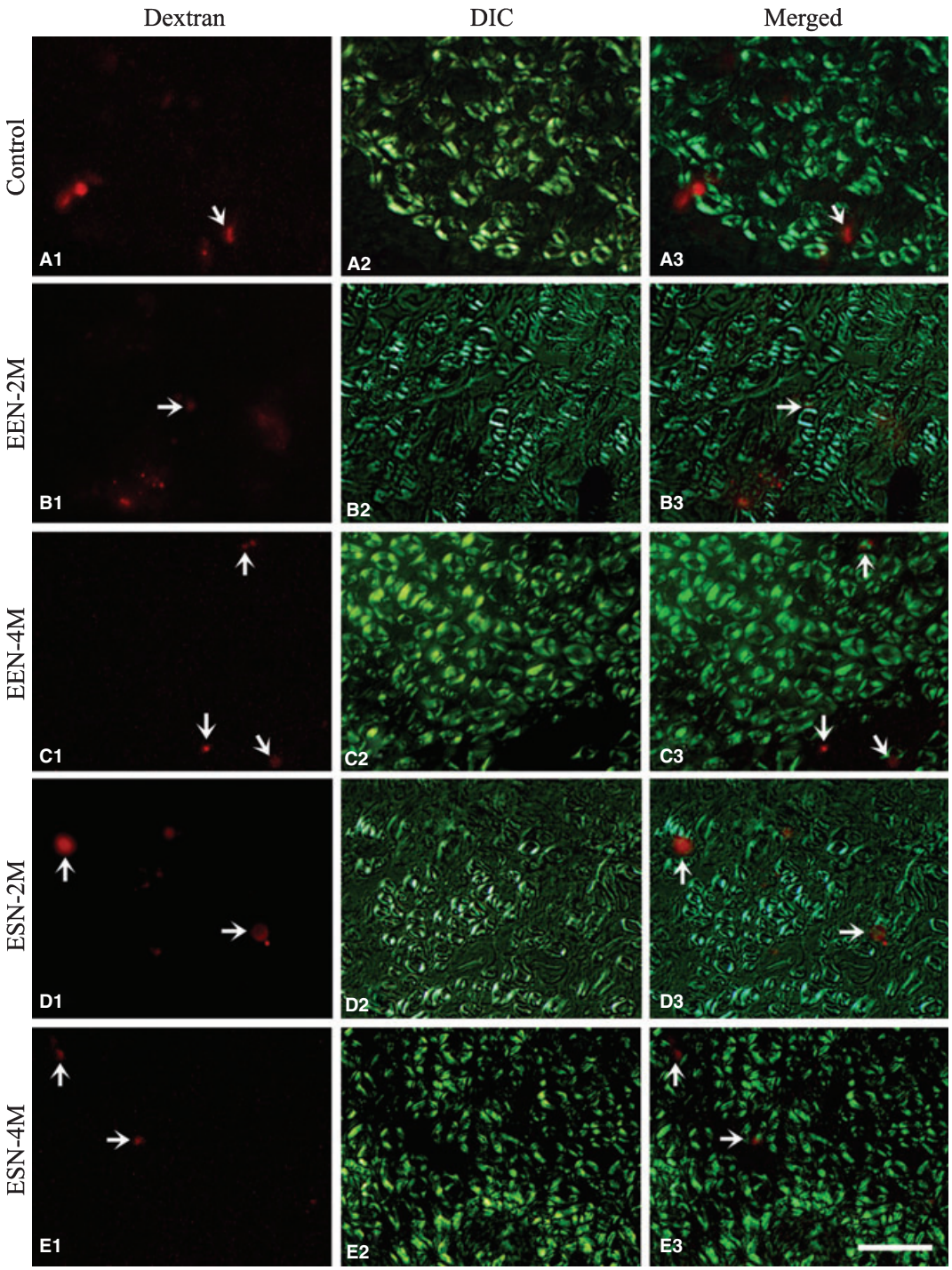

Fig. 9 Anterograde tracing of sensory fibers traveling into the recipient nerve. The anterograde tracer was applied to the C7 DRG. A fluorescence image of the anterograde tracer dextran (left column) and DIC micrographs (middle column) of the same representative area of cross-sections of the recipient nerve of different groups are illustrated as labeled. The right column shows superimposed images of the two photographs on the left. Arrows point to the locations of representative fluorescence areas that contain labeled sensory axons. Scale bar = 10 μm.

myelin thickness of the reinnervating axons at ESN-6 months remained rather scattered, a pattern resembling that of the EEN-2 month animals but with apparent scarcity of large-size fibers. The predominance of small fibers, the low density of MEPs and the small amplitudes of CMAPs indicate that the ESN-6 months repaired nerve functions far below the level of control nerve and could still be reorganizing.

Among the several parameters we used to assess reinnervation following neurorrhaphy, retrograde labeling of

motoneurons, number of axons and their distribution based on diameters, correlation between axon diameters and myelin thickness and density of MEPs in the target muscle correlate well with the recovery of CMAP. However, the results of the forelimb grooming test were not satisfactory in this regard and forelimb grooming response appeared to be more complex than operation of elbow and shoulder flexion alone. In our hands, forelimb grooming score reliably reflected the initial recovery response of elbow flexion to reach the snout or below the eye, the lower score range of the test, in the early months following EEN and ESN, but appeared not to correlate with the recovery in the higher score range, consistent with our concern that higher score behavior could be complicated by head and neck bending.

In conclusion, we assessed the reconnection of rat McN to UN in EEN and ESN configurations. EEN was quicker and better than ESN in restoring lost function, but at the expense of donor function. ESN, although slower, ultimately resulted in recovery of modest control of the lost function. These differences appeared to stem largely from the fact that EEN deals with regeneration of severed axons, whereas ESN deals with collateral sprouting of intact donor axons. In light of this and recent findings that neurotrophic or immunosuppressive substances appear to be involved (Fortes et al. 1999) or might enhance (McCallister et al. 2001; Lykissas et al. 2007; Chen et al. 2009) the sprouting and growth of nerve fibers following neurorrhaphy, ESN in combination with measures to speed up the collateral sprouting of donor axons and their maturation should be explored further in the future.

Acknowledgements

We thank the late Dr J.-W. Yin of the Kaohsiung Chang Gung Memorial Hospital for advice on surgical technique and for discussion of results, and Professor Dr E. A. Ling of the National University of Singapore for reading the manuscript. This work was supported by grants from the National Science Council of Taiwan to J.-R. Chen (NSC-97-2313-B-005-045), Y.-J. Wang (NSC-97-2320-B-007) and G.-F. Tseng (NSC97-2320-B-320-006); and grants from the Tzu-Chi University (TCIRP-95003) to G.-F. Tseng and Y.-J. Wang.

References

Akeda K, Hirata H, Matsumoto M, et al. (2006) Regenerating axons emerge far proximal to the coaptation site in end-to-side nerve coaptation without a perineurial window using a T-shaped chamber. *Plast Reconstr Surg* **117**, 1194–1203.

Beris A, Lykissas M, Korompilias A, et al. (2007) End-to-side nerve repair in peripheral nerve injury. *J Neurotrauma* **24**, 909–916.

Bertelli JA, Ghizoni MF (2006) Concepts of nerve regeneration and repair applied to brachial plexus reconstruction. *Microsurgery* **26**, 230–244.

Bertelli JA, Mira JC (1993) Nerve repair using freezing and fibrin glue: immediate histologic improvement of axonal coaptation. *Microsurgery* **14**, 135–140.

Bertelli JA, dos Santos AR, Calixto JB (1996) Is axonal sprouting able to traverse the conjunctival layers of the peripheral nerve? A behavioral, motor, and sensory study of end-to-side nerve anastomosis. *J Reconstr Microsurg* **12**, 559–563.

Chen JR, Wang YJ, Tseng GF (2003) The effect of epidural compression on cerebral cortex: a rat model. *J Neurotrauma* **20**, 767–780.

Chen B, Song Y, Liu Z (2009) Promotion of nerve regeneration in peripheral nerve by short-course FK506 after end-to-side neurorrhaphy. *J Surg Res* **152**, 303–310.

Chuang TY, Chiu FY, Tsai YA, et al. (2002) The comparison of electrophysiologic findings of traumatic brachial plexopathies in a tertiary care center. *Injury* **33**, 591–595.

Crews LL, Wigston DJ (1990) The dependence of motoneurons on their target muscle during postnatal development of the mouse. *J Neurosci* **10**, 1643–1653.

Fortes WM, Noah EM, Liuzzi FJ, et al. (1999) End-to-side neurorrhaphy: evaluation of axonal response and upregulation of IGF-I and IGF-II in a non-injury model. *J Reconstr Microsurg* **15**, 449–457.

Guntinas-Lichius O, Hundeshagen G, Paling T, et al. (2007) Impact of different types of facial nerve reconstruction on the recovery of motor function: an experimental study in adult rats. *Neurosurgery* **61**, 1276–1283. Discussion 1283–5.

Haas CA, Donath C, Kreutzberg GW (1993) Differential expression of immediate early genes after transection of the facial nerve. *Neuroscience* **53**, 91–99.

Hayashi A, Yanai A, Komuro Y, et al. (2004) Collateral sprouting occurs following end-to-side neurorrhaphy. *Plas Reconstr Surg* **116**, 129–137.

Hayashi A, Pannucci C, Moradzadeh A, et al. (2008) Axotomy or compression is required for axonal sprouting following end-to-side neurorrhaphy. *Exp Neurol* **211**, 539–550.

Kanje M, Arai T, Lundborg G (2000) Collateral sprouting from sensory and motor axons into an end to side attached nerve segment. *Neuroreport* **11**, 2455–2459.

Liu CL, Wang YJ, Chen JR, et al. (2002) Parvalbumin-containing neurons mediate the feedforward inhibition of rat rubrospinal neurons. *Anat Embryol* **205**, 245–254.

Liu PH, Yang LH, Wang TY, et al. (2006) Proximity of lesioning determines response of facial motoneurons to peripheral axotomy. *J Neurotrauma* **23**, 1857–1873.

Lundborg G (2005). *Nerve Injury and Repair*. Edinburgh: Churchill Livingstone.

Lutz BS, Chuang DC, Hsu JC, et al. (2000) Selection of donor nerves – an important factor in end-to-side neurorrhaphy. *Br J Plast Surg* **53**, 149–154.

Lykissas MG, Sakellariou E, Vekris MD, et al. (2007) Axonal regeneration stimulated by erythropoietin: an experimental study in rats. *J Neurosci Methods* **164**, 107–115.

Matsumoto M, Hirata H, Nishiyama M, et al. (1999) Schwann cells can induce collateral sprouting from intact axons: experimental study of end-to-side neurorrhaphy using a Y-chamber model. *J Reconstr Microsurg* **15**, 281–286.

McCallister WV, Tang P, Smith J, et al. (2001) Axonal regeneration stimulated by the combination of nerve growth factor and ciliary neurotrophic factor in an end-to-side model. *J Hand Surg [Am]* **26**, 478–488.

Nagano A (1998) Treatment of brachial plexus injury. *J Orthop Sci* **3**, 71–80.

Oberlin C, Beal D, Leechavengvongs S, et al. (1994) Nerve transfer to biceps muscle using a part of ulnar nerve for C5-C6

avulsion of the brachial plexus: anatomical study and report of four cases. *J Hand Surg [Am]* **19**, 232–237.

Samal F, Haninec P, Raska O, et al. (2006) Quantitative assessment of the ability of collateral sprouting of the motor and primary sensory neurons after the end-to-side neurorrhaphy of the rat musculocutaneous nerve with the ulnar nerve. *Ann Anat* **188**, 337–344.

Schmalbruch H (1987) Loss of sensory neurons after sciatic nerve section in the rat. *Anat Rec* **219**, 323–329.

Stoll G, Muller HW (1999) Nerve injury, axonal degeneration and neural regeneration: basic insights. *Brain Pathol* **9**, 313–325.

Tham SK, Morrison WA (1998) Motor collateral sprouting through an end-to-side nerve repair. *J Hand Surg [Am]* **23**, 844–851.

Tseng GF, Lan CT, Shieh JY, et al. (1996) Tracing in living CNS tissue slices with dextran. *Neurosci Protoc* **50**, 1–13.

Tung TH, Novak CB, Mackinnon SE (2003) Nerve transfers to the biceps and brachialis branches to improve elbow flexion strength after brachial plexus injuries. *J Neurosurg* **98**, 313–318.

Ulkur E, Yuksel F, Acikel C, et al. (2003) Comparison of functional results of nerve graft, vein graft, and vein filled with muscle graft in end-to-side neurorrhaphy. *Microsurgery* **23**, 40–48.

Viterbo F, Trindade JC, Hoshino K, et al. (1992) Latero-terminal neurorrhaphy without removal of the epineural sheath. Experimental study in rats. *Rev Paul Med* **110**, 267–275.

Viterbo F, Trindade JC, Hoshino K, et al. (1994) End-to-side neurorrhaphy with removal of the epineurial sheath: an experimental study in rats. *Plast Reconstr Surg* **94**, 1038–1047.

Wang YJ, Ho HW, Tseng GF (2000) Fate of the supraspinal collaterals of cord-projection neurons following upper spinal axonal injury. *J Neurotrauma* **17**, 231–241.

Zhang Z, Johnson EO, Vekris MD, et al. (2006) Long-term evaluation of rabbit peripheral nerve repair with end-to-side neurorrhaphy in rabbits. *Microsurgery* **26**, 245–252.